Supplementary information for

Berry curvature origin of the thickness dependent anomalous Hall effect in a ferromagnetic Weyl semimetal

Yao Zhang[1,2,3], Yuefeng Yin[4,5], Guy Dubuis[1,2], Tane Butler[1], Nikhil V. Medhekar[4,5] and Simon Granville[1,2]

[1]Robinson Research Institute, Victoria University of Wellington, Wellington, New Zealand.
[2]MacDiarmid Institute for Advanced Materials and Nanotechnology, Wellington, New Zealand.
[3]School of Chemical and Physical Sciences, Victoria University of Wellington, Wellington, New Zealand.
[4]Department of Materials Science Engineering, Monash University, Clayton, Australia.
[5]ARC Centre of Excellence in Future Low Energy Electronics, Monash University, Clayton, Australia.

Supplementary Note 1

Anomalous Hall effect and magnetic hysteresis loop of the Co_2MnGa film

Supplementary Figure 1 presents anomalous Hall effect and magnetic hysteresis loop along out-of-plane of the 50 nm Co_2MnGa film. The saturation field of magnetization along out-of-plane is 1 T in line with the electrical transport measurement. What's more, the loop shows a very small square loop with a coercive field $\mu_0 H_c$ = 23.6 mT which is quite small compared with saturation field. One can obtain obvious knots in the resistivity curve which indicating the out-of-plane magnetization component seen in the magnetization measurements.

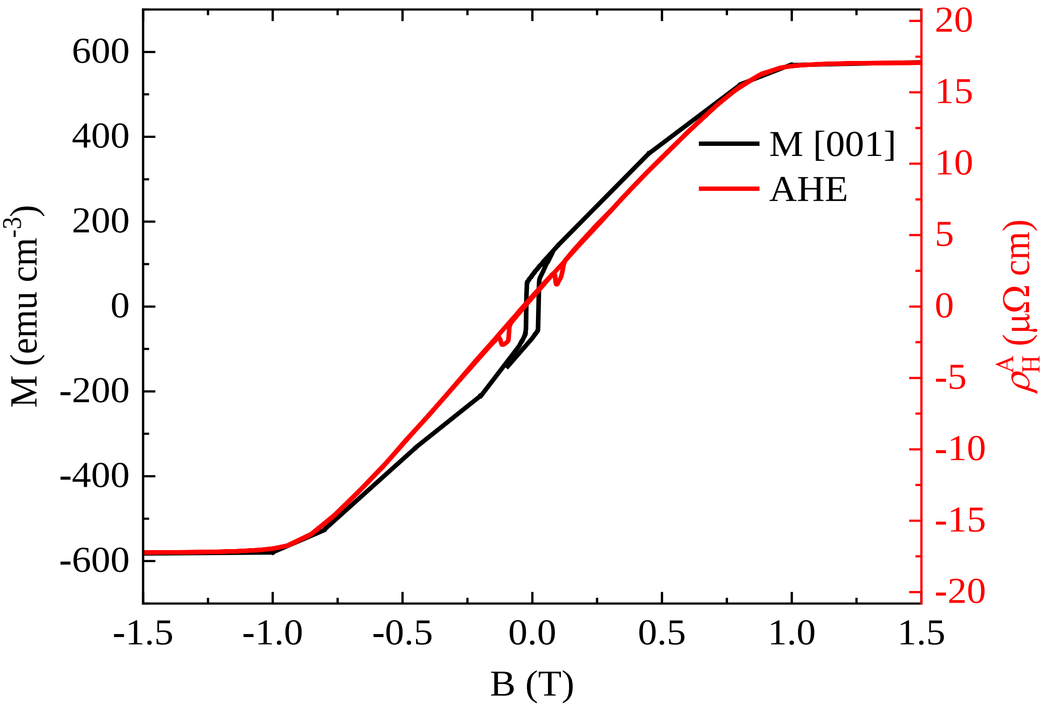

Supplementary Figure 1. Anomalous Hall effect and magnetic hysteresis loop along out-of-plane of the 50 nm Co_2MnGa film measured at 300 K.

Supplementary Note 2

Temperature dependence of magnetization and electrical transport of the Co_2MnGa film

Supplementary Figure 2 presents the temperature dependence of magnetization for the 50 nm Co_2MnGa film. It still shows ferromagnetism at 400 K. The Curie temperature is approximately 800 K as shown by the fit with the extended Bloch law $M = M_s\left(1 - aT^{5/2}\right)$ [1], which is slightly larger than the bulk value ~700 K[2].

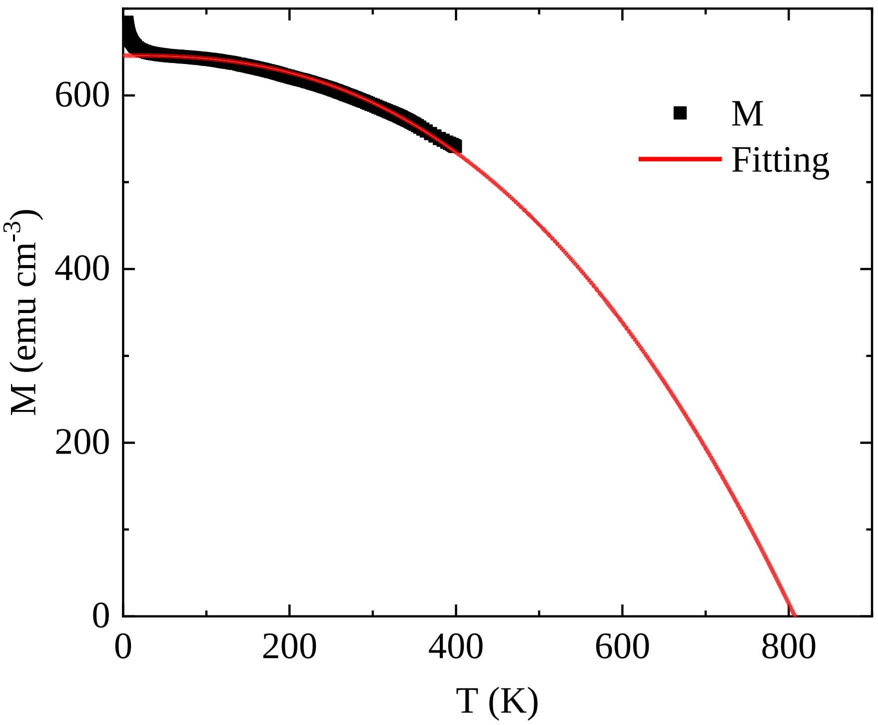

Supplementary Figure 2. Temperature dependence of magnetization for the 50 nm Co_2MnGa film measured from 5 K to 400 K along [110] direction with 50 mT.

Supplementary Figure 3 shows the ρ_{xx} and ρ_{xy} as a function of temperature from 3 K to 300 K for Co_2MnGa (5-50 nm). The ρ_{xx} is in the range of 167-208 μΩ cm at 300 K for Co_2MnGa (5-50 nm). Especially of note, the ρ_{xx} of 10 nm Co_2MnGa films is almost same as one of 50 nm. This small difference suggests that all films show similar crystalline quality. What's more, the residual resistivity ratios (see inset of Supplementary Figure 3a) of all Co_2MnGa films in our results are similar and even slightly larger than films from previous reports in which a good $L2_1$-order structure has been confirmed (e.g. 30 nm film in Supplementary Ref. [3] and 80 nm in Supplementary Ref. [4]).

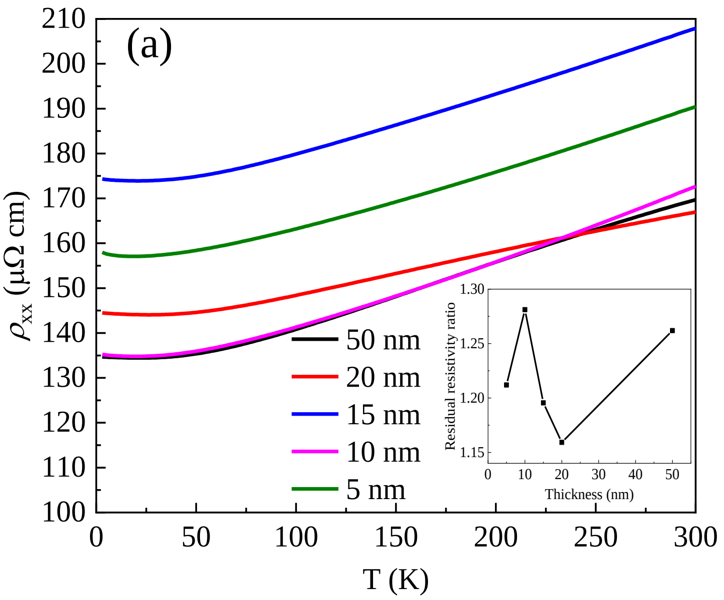

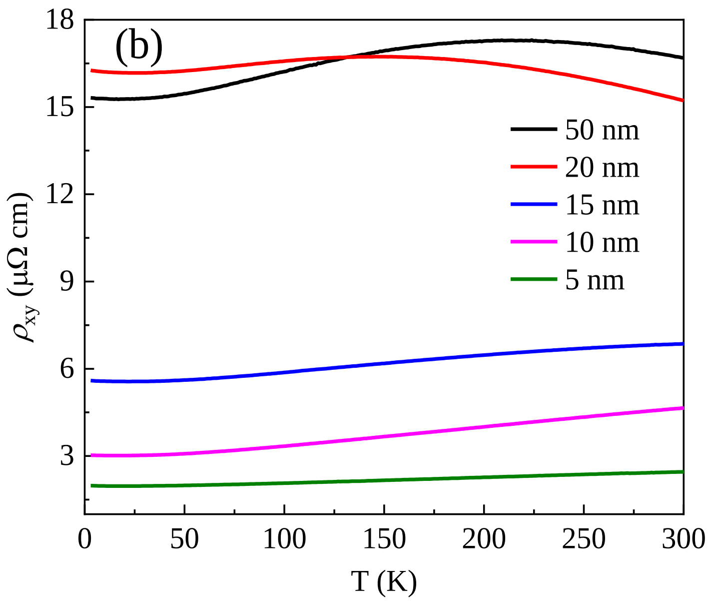

Supplementary Figure 3. (a) Longitudinal resistivity without field as a function of temperature from 3 K to 300 K for Co_2MnGa (5-50 nm). The inset shows the residual resistivity ratio ($\rho_{xx(300K)}/\rho_{xx(residual)}$) as a function of thickness. (b) Anomalous Hall resistivity cooling down in 9 T as a function of temperature from 3 K to 300 K for Co_2MnGa (5-50 nm).

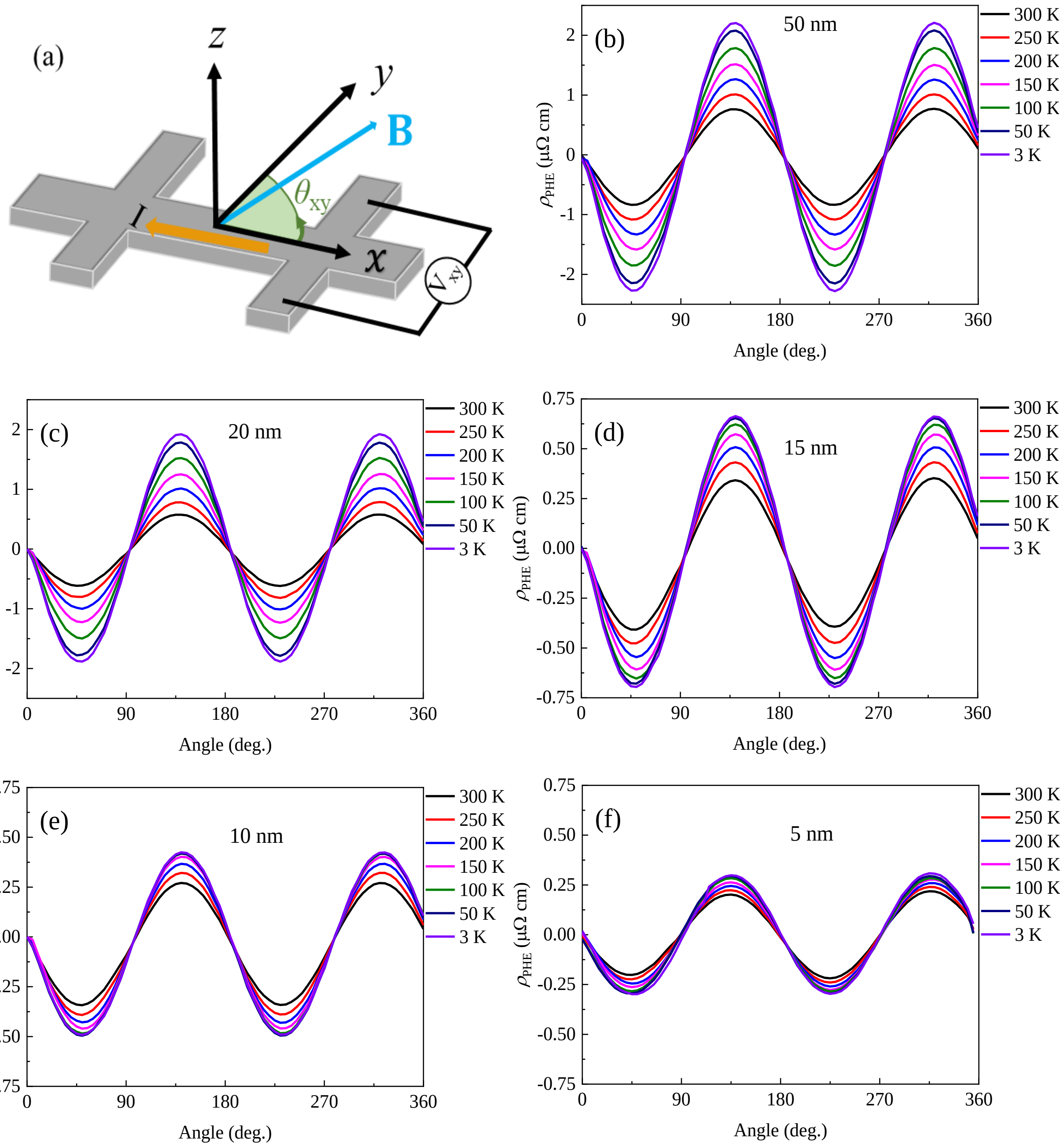

Supplementary Figure 4. Angular dependence of planar Hall resistivity for various thickness of Co_2MnGa film. (a) Schematic of measurement geometry. The angle θ_{xy} represents the angle between the rotating field and *x*-axis when the field rotates from *x*-axis to *y*-axis in the *xy* plane. Current is along the [100] direction of Co_2MnGa. (b)-(f) planar Hall resistivity as a function of angle, θ_{xy}, measured from 300 K and 3 K under a magnetic field of 9 T for 50, 20, 15, 10 and 5 nm Co_2MnGa film, respectively.

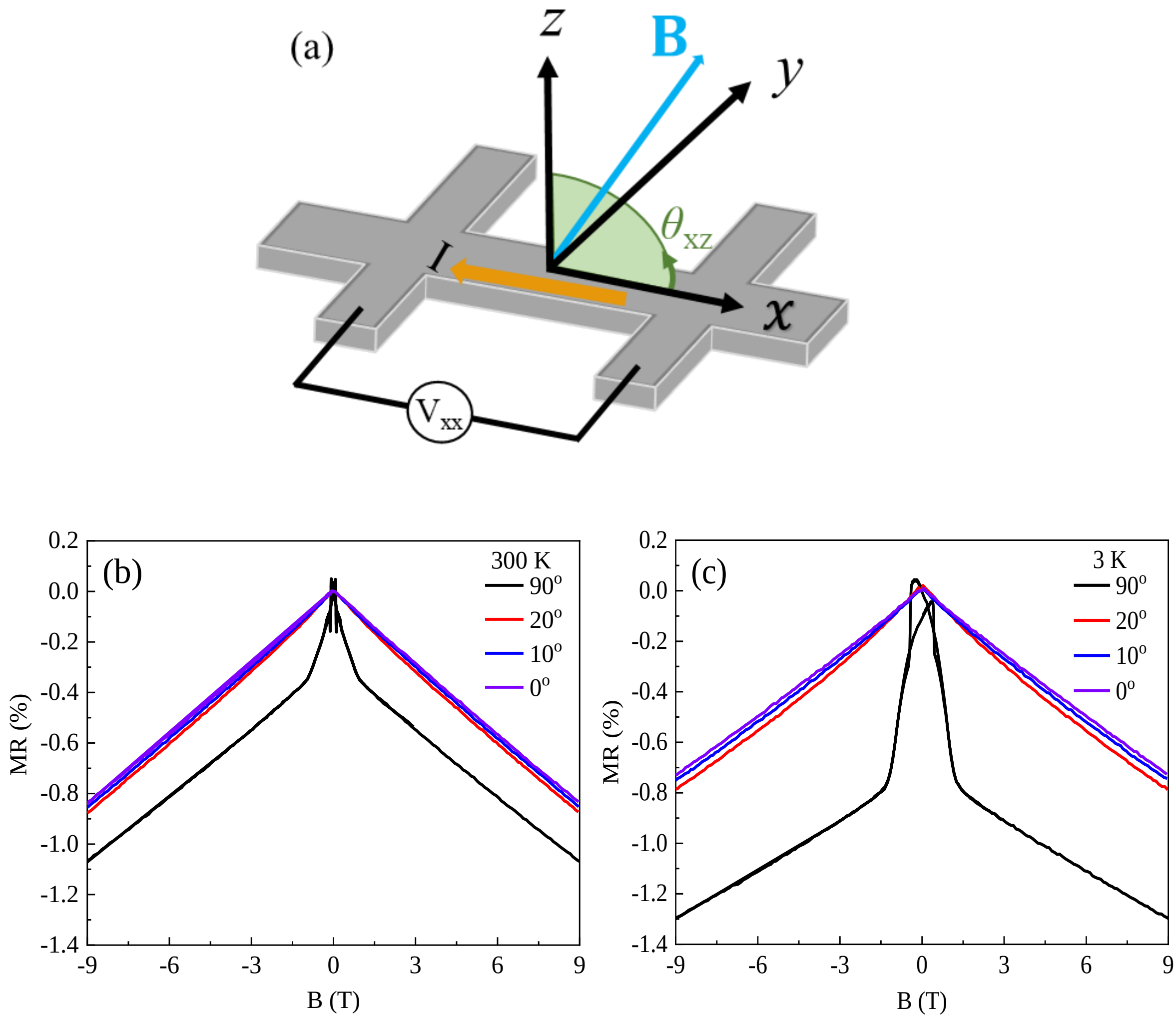

Supplementary Figure 5. Magnetoresistance (MR) ratio of the 50 nm Co_2MnGa film. (a) Schematic of measurement geometry. The angle θ_{xz} represents the angle between the rotating field and *x*-axis when the field rotates from *x*-axis to *z*-axis in the *xz* plane. Current is along the [100] direction of Co_2MnGa. (b) and (c) MR ratio as a function of magnetic field measured at 300 K and 3 K with various angles, θ_{xz}, respectively.

Supplementary Note 3

Surface band structure of Co_2MnGa

Supplementary Figure 6 presents the Co-terminated and MnGa-terminated surface electronic band structure of 4.9 nm and 50.1 nm Co_2MnGa. Some surface bands from minority spin electrons around the Fermi level are highly isolated from the bulk counterparts independent of film thickness, while the surface character of bands from majority spins, covering by bulk band structure, shows significant changes when film thickness decreases. This could explain the different extent of Berry curvature reduction between majority and minority spin electrons.

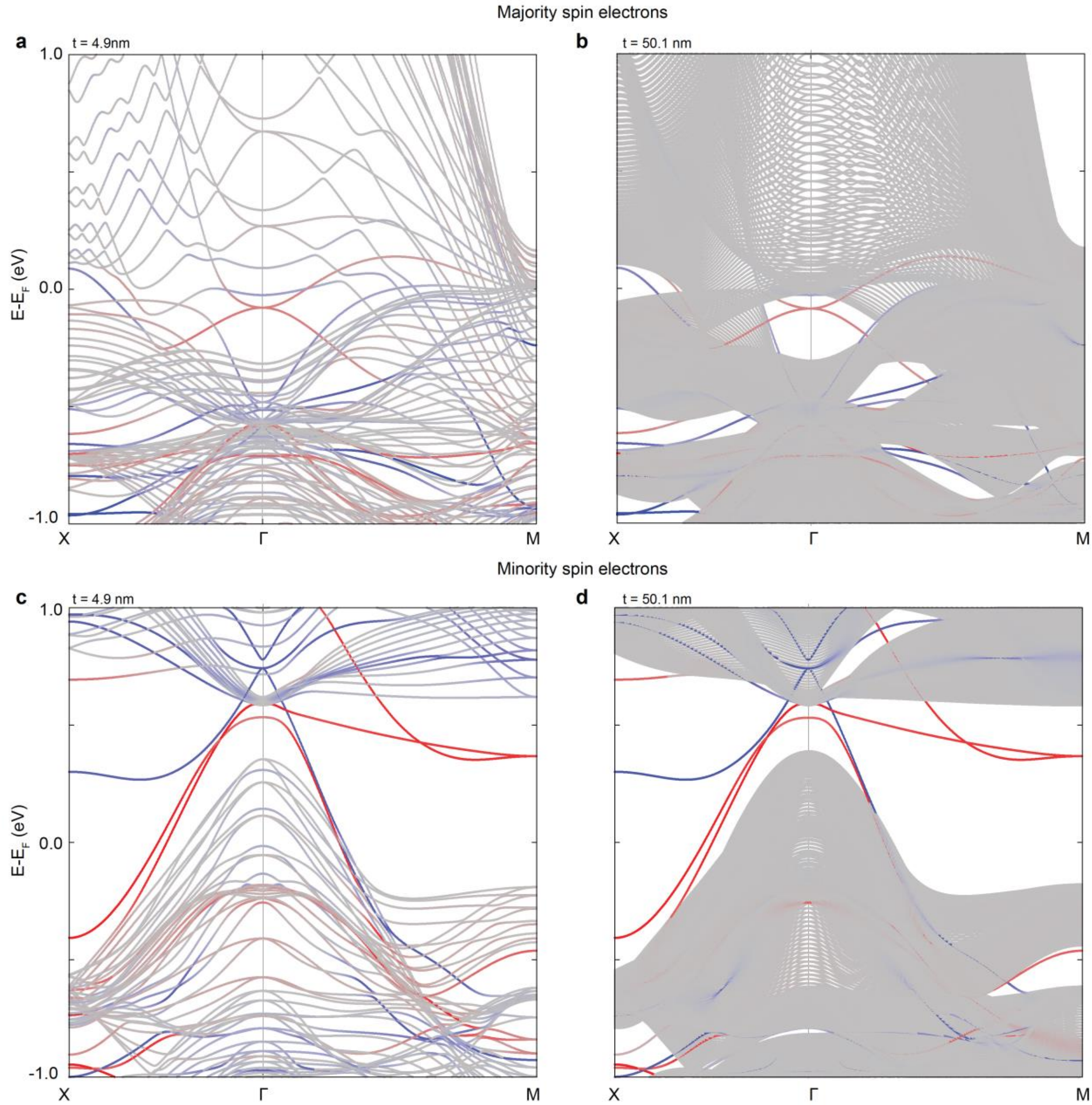

Supplementary Figure 6. (001) Surface band structure of Co_2MnGa. The grey bands are bulk bands. The red and blue bands are from Co-terminated surface and MnGa-terminated surface, respectively. (a) and (b) show surface band structure of majority spin electrons for Co_2MnGa thin films of 4.9 nm and 50.1 nm. (c) and (d) show corresponding surface band structure of minority spin electrons.

Supplementary Note 4

The σ_{xy} dependent anomalous Hall angle

Comparison of our anomalous Hall angle results and previously reported data for other magnetic thin films was performed. The reported data were taken from references that can be found in supplementary Table 1.

Materials	$\boldsymbol{\sigma_{xx}}$**(Ω^{-1} cm^{-1})**	$\boldsymbol{\sigma_{xy}}$**(Ω^{-1} cm^{-1})**	$\boldsymbol{\theta_H}$**(%)**	**Refs.**
MnGa	5100	288	5.71	5
Mn_2Ru_xGa	2900	220	7.7	6
Co_2TiSn	6578.5	51.9	0.79	7
$Co_2Ti0_{.6}V_{0.4}Sn$	1602.4	13.9	0.87	7
$L1_0$-FePt	37900	1250	3.3	5
TbCo	25000	800	3.2	5
SmFe	6600	317	4.8	5
FeGd	5111	295	5.8	8
GaMnAs	2200	147	6.6	5
$SrRuO_3$	20000	200	1	5
Fe	43600	1134	2.6	9
Co, Ni	100000	500	0.06	9
Gd	500000	1000	0.2	9
Pt/Py	23800	380	1.6	10
Pt/Co multilayers	24376	595	2.3	11
$Mn_5Ge_3C_{0.8}$	3326	155	4.7	12
$Co_3Sn_2S_2$	3850	770	20	13
Co_2MnGa	**6805.2**	**774.4**	**11.4**	**Present work**

Supplementary Table 1. Summary of σ_{xx}, σ_{xy}, and θ_H of magnetic thin films. Only the maximum values of θ_H are adopted here.

Supplementary References

1. Köbler, U. & Hoser, A. Magnetism of powder samples and of single crystals. *J. Magn. Magn. Mater.* **349**, 88–94 (2014).
2. Webster, P. J. Magnetic and chemical order in Heusler alloys containing cobalt and manganese. *J. Phys. Chem. Solids* **32**, 1221–1231 (1971).
3. Wang, Q., Wen, Z., Kubota, T., Seki, T. & Takanashi, K. Structural-order dependence of anomalous Hall effect in Co_2MnGa topological semimetal thin films. *Appl. Phys. Lett.* **115**, 252401 (2019).
4. Markou, A. *et al.* Thickness dependence of the anomalous Hall effect in thin films of the topological semimetal Co_2MnGa. *Phys. Rev. B* **100**, 054422 (2019).
5. Liu, E. *et al.* Giant anomalous Hall effect in a ferromagnetic kagome-lattice semimetal. *Nat. Phys.* **14**, 1125–1131 (2018).
6. Thiyagarajah, N. *et al.* Giant spontaneous Hall effect in zero-moment Mn_2Ru_xGa. *Appl. Phys. Lett.* **106**, 122402 (2015).
7. Hu, J. *et al.* Anomalous Hall and Nernst Effects in Co_2TiSn and $Co_2Ti_{0.6}V_{0.4}Sn$ Heusler Thin Films. *Phys. Rev. Appl.* **10**, 044037 (2018).
8. McGuire, T. R., Gambino, R. J. & Taylor, R. C. Hall effect in amorphous thin-film magnetic alloys. *J. Appl. Phys.* **48**, 2965–2970 (1977).
9. Miyasato, T. *et al.* Crossover behaviour of the anomalous Hall effect and anomalous Nernst effect in itinerant ferromagnets. *Phys. Rev. Lett.* **99**, 086602 (2007).
10. Zhang, Y. Q., Sun, N. Y., Che, W. R., Shan, R. & Zhu, Z. G. Origin of enhanced anomalous Hall effect in ultrathin Pt/permalloy bilayers. *AIP Adv.* **6**, 025214 (2016).
11. Moritz, J., Rodmacq, B., Auffret, S. & Dieny, B. Extraordinary Hall effect in thin magnetic films and its potential for sensors, memories and magnetic logic applications. *J. Phys. D: Appl. Phys.* **41**, 135001 (2008).
12. Sürgers, C., Fischer, G., Winkel, P. & Löhneysen, H. v. Magnetotransport in ferromagnetic Mn_5Ge_3, $Mn_5Ge_3C_{0.8}$, and $Mn_5Si_3C_{0.8}$ thin films. *Phys. Rev. B* **90**, 104421 (2014).

13. Fujiwara, K. *et al*. Ferromagnetic $Co_3Sn_2S_2$ thin films fabricated by co-sputtering. *Jpn. J. Appl. Phys.* **58**, 050912 (2019).